

Space-charge-limited currents in ice

V. F. Petrenko and I. A. Ryzhkin

Institute of Solid-State Physics, Academy of Sciences of the USSR

(Submitted 2 December 1983)

Zh. Eksp. Teor. Fiz. **87**, 558–569 (August 1984)

A theoretical and experimental study is made of space-charge-limited currents in ice. Comparison of the theoretical and experimental results yields a value of the mobility of the most mobile charge carriers in ice, viz., the H_3O^+ ions.

INTRODUCTION

The extensive physical research on ice in the last twenty-five years has been motivated both by an obvious practical importance and by the extremely unusual properties of ice. For example, the behavior of ice in electric fields differs strongly from the behavior of ordinary electronic insulators and semiconductors. This is because the electrical properties of ice are due to the motion of protons, not electrons.

The results of the research of previous years can be summarized in the following model for ice. In the most common modification, hexagonal ice, the oxygen atoms form a regular lattice of the wurtzite type (Fig. 1).^{1,2} Every oxygen atom has four nearest neighbors at a distance $r_{\text{OO}} = 2.76 \text{ \AA}$. Every O–O bond has two potential wells for the protons at a distance of 1 \AA from the oxygen atoms. The distribution of the $2N$ protons (N is the number of H_2O molecules in the crystal) over the $4N$ sites satisfies the Bernal-Fowler (BF) rule³:

- a) there is one proton in every bond;
- b) there are two protons close to every oxygen atom.

Despite these restrictions, the number of different proton configurations (BF configurations) is large. Pauling⁴ estimated their number as $(3/2)^N$ and, assuming that all the BF configurations have the same probability, obtained the residual entropy of ice as $S_0 = kN \ln(3/2)$ (k is the Boltzmann constant). Nagle⁵ subsequently carried out more-exact calculations but found only an unimportant difference from the crude Pauling approximation. The estimates of the residual entropy are in excellent agreement with the experimental results of Gisuque and Stout⁶; this agreement (together with other facts) confirms the above description of the protonic structure of ice.

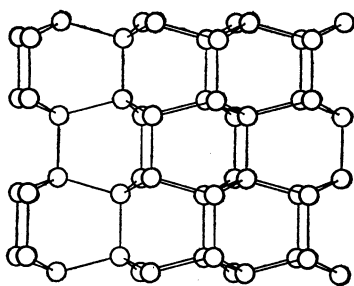


FIG. 1. Structure of hexagonal ice. The circles indicate the oxygen atoms; the proton positions in the bonds are not shown.

One cannot pass from one BF configuration to another by individual proton moves without breaking the BF rules. Therefore, in an ideal BF configuration the transport of charge by protons and the reorientation of the ice molecules cannot occur. However, one can create certain defects, known as D and L defects (which break rule a) and H_3O^+ and OH^- defects (which break rule b), whose motion makes it possible to go between different BF configurations (Fig. 2).^{7,8} Working from these ideas, Jaccard^{9,10} created a phenomenological model for the electrical properties of ice; this model was recently refined by Hubmann.¹¹

Though confirmed in its general features by many experiments (see, e.g., Ref. 12), this model suffers from the lack of experimentally measured values of the mobilities μ_i and concentrations n_i of the H_3O^+ , OH^- , D , and L defects. In fact, all the quantities which have been measured to date (the dielectric constant ϵ and the electrical conductivity σ) contain the products $\mu_i n_i$, and no one has yet been able to measure the Hall constant because of the low mobilities. Therefore, it is important to employ new methods for studying the electrical properties of ice.

For many materials the study of electron injection from contacts and the measurement of the space-charge-limited currents arising thereby are effective methods for studying such parameters as the mobility and lifetime of the current carriers, the concentration of defects, and the nature of the traps. The power of this method has been demonstrated particularly clearly for semiconductors.^{13,14} For this reason it seems attractive to apply the method of injection currents to the study of a protonic semiconductor—ice. However, many of the theoretical concepts developed for electronic conduc-

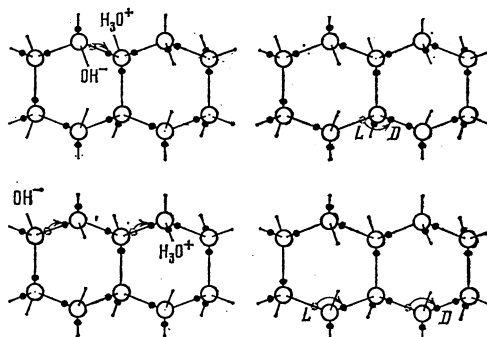


FIG. 2. Diagram illustrating the formation and motion of H_3O^+ , OH^- , D , and L defects.

tors do not apply to ice. Therefore, it is necessary to first make a theoretical study of space-charged-limited currents in ice in order to correctly analyze the experimental results. The present paper is designed to address this problem. In Part I we make a theoretical study of space-charged-limited currents in ice. In Part II we describe the experimental technique and present results which are interpreted on the basis of the theory developed in Part I.

PART I. THE THEORY OF SPACE-CHARGE-LIMITED CURRENTS IN ICE

§1. Basic equations

Let us consider an ice crystal of thickness l , to which a dc voltage V is applied at time $t = 0$. The contacts at $x = 0$ and $x = l$ will be assumed ideal, which means that there are infinite concentrations of current carriers at the injecting contact at $x = 0$ and that there is no voltage drop across the collecting contact at $x = l$. Our problem is to evaluate the dependence of the electric current I on the voltage V and thickness l .

We denote the defects H_3O^+ , OH^- , D , and L by subscripts $i = 1, 2, 3$, and 4 , respectively. The defect concentrations n_i and current densities j_i satisfy the continuity equations

$$\partial n_i / \partial t + \text{div } j_i = 0. \quad (1)$$

Equations (1) apply only in the absence of chemical reactions or, if reactions are present, under the condition that a chemical equilibrium is maintained at any instant in time. Otherwise, the right-hand side of equations (1) would contain the rate of formation of particles in the chemical reactions.

The electric field is determined by Poisson's equation

$$\text{div } E = 4\pi\rho, \quad (2)$$

where ρ is the total charge density. Let us write the charge density as

$$\rho = \rho_d + \rho_p,$$

where ρ_d is the charge density of the defects and ρ_p is the polarization charge density of the water molecules with the exclusion of the polarization charge due to their permanent dipole moment. At time $t = 0$ we have $\rho = \rho_d = \rho_p = 0$. Hence, for $\rho_d(t)$ at $t \rightarrow \infty$ we get

$$\begin{aligned} \rho_d(\infty) &= - \lim_{v \rightarrow 0} v^{-1} \int_0^\infty dt \oint_s j ds = - \sum_{i=1}^4 e_i \lim_{v \rightarrow 0} v^{-1} \int_0^\infty dt \\ &\times \int_v \text{div } j_i dv = + \sum_{i=1}^4 e_i \int_0^\infty dt \frac{\partial n_i}{\partial t} = + \sum_{i=1}^4 e_i \delta n_i. \end{aligned} \quad (3)$$

Here v is a physically infinitesimal volume, s is its surface area, ds is an element of area, $\delta n_i = n_i(\infty) - n_i(0)$, j is the electric current density, by definition equal to

$$j = \sum_{i=1}^4 e_i j_i, \quad (4)$$

and e_i are the effective charges of the defects. From the above definition it is seen that the effective charge of defect i

is equal to the charge e_i which, in moving through a distance δr_i , would cause the same electric current as do the actual proton and electron motions necessary for a displacement of the defect by an amount δr_i . It can be shown that the e_i have the properties

$$e_1 = -e_2, \quad e_3 = -e_4, \quad e_1 + e_3 = e,$$

where e is the proton charge. The charge density ρ_p can be taken into account by introducing a high-frequency dielectric constant $\epsilon = 3.17$. As a result, Poisson's equation assumes the form

$$\text{div } E = \frac{4\pi}{\epsilon} \sum_{i=1}^4 e_i \delta n_i. \quad (5)$$

In the Jaccard theory the state of the proton system is characterized by a configuration vector Ω , which has the following physical meaning. If we consider the O-O bonds parallel to a certain direction z , the protons in these bonds can be found in two positions: 1 and 2 (suppose $z_1 > z_2$). For a completely random BF configuration the numbers of bonds in states 1 and 2 are equal: $N_1 = N_2$. The corresponding component Ω_z of the configuration vector is zero in this case. If, however, $N_1 > N_2$, then the configuration is partially ordered, and $\Omega_z \neq 0$. Because the defects change their state in moving along the bond,⁹ the vector Ω is related to the fluxes of the particles. One can define Ω as¹⁰

$$\Omega = \int_0^t dt' \sum_{i=1}^4 \eta_i j_i(t'), \quad (6)$$

where $\eta_1 = 1$, $\eta_2 = -1$, $\eta_3 = -1$, and $\eta_4 = 1$ take into account the character of the orientation of the bond by defects 1, 2, 3, and 4. Taking the divergence of Eq. (6), using Eq. (1), and passing to the limit $t \rightarrow \infty$, one easily obtains, for steady-state processes,

$$\text{div } \Omega = - \sum_{i=1}^4 \eta_i \delta n_i. \quad (7)$$

Finally, we have the phenomenological equations for the fluxes:

$$j_i = (e_i E - \eta_i \Phi \Omega) \frac{\mu_i n_i}{|e_i|} - D_i \text{grad } n_i. \quad (8)$$

Here $\Phi = 3.85 r_{OO} kT$ (Ref. 11), where T is the temperature and D_i are the diffusion coefficients.

In Eq. (8) the term $\eta_i \Phi \Omega$ enters as a sort of force acting on the defects. This force is due to the fact that in an oriented lattice ($\Omega \neq 0$), random jumps of defects give rise to a directed flux of these defects.

From now on we shall consider only the steady, one-dimensional case, in which all the quantities depend only on x . We shall everywhere neglect the diffusion term $D_i \text{grad } n_i$, since it is small throughout almost the entire crystal, except for a narrow region near the injecting contact, and it would only lead to a small correction to the characteristic $I(V, l)$. Equations (1), (5), (7), and (8) enable one to find E , Ω , j_i , and n_i , and with the aid of Eq. (4) and the condition

$$V = \int_0^l E(x) dx \quad (9)$$

one can find the volt-ampere characteristic $I(V, I)$.

§2. Boundary conditions and restrictions on the possible forms of steady-state injection

We shall consider contacts which are able to exchange protons with ice. A single proton upon injection into the ice lattice immediately forms two defects: H_3O^+ and D . Similarly, one "proton hole" formed as a result of the extraction of a proton into the contact is equivalent to a pair of defects: OH^- and L . Thus, the charge carriers usually come off the contacts in pairs: (1,3) and (2,4). However, the relatively immobile members of the pairs (presumably the OH^- and D defects) can then remain trapped by the surface or by traps until they are annihilated. This circumstance makes it possible to have any combination of injected carriers for contacts capable of exchanging protons with the ice.

For the case of the double injection (1,3), allowance for what we have said and for the stipulated ideality of the contact gives for the boundary condition at the proton-injecting contact

$$\delta n_1 \rightarrow \infty, \quad \delta n_3 \rightarrow \infty, \quad \delta n_3 / \delta n_1 \rightarrow r \quad (10)$$

as $x \rightarrow 0$. Here r is some constant.

Let us now consider the restrictions imposed by Eqs. (6) and (8) on the possible forms of steady injection. Because Ω is independent of t in the steady-state case, we have from Eq. (6)

$$\sum_{i=1}^4 \eta_{ij} j_i = 0. \quad (11)$$

From this we see immediately that mono-injection, with a current of only one type of defect, is impossible.

Let us now consider the possibility of injection (1,2). This means that $j_1 \neq 0$, $j_2 \neq 0$, $j_3 = j_4 = 0$. From Eq. (8) we obtain, without the diffusion term,

$$\begin{aligned} j_1 &= \frac{\mu_1 n_1}{|e_1|} (e_1 E - \Phi \Omega) \neq 0, \\ j_2 &= \frac{\mu_2 n_2}{|e_2|} (e_2 E + \Phi \Omega) \neq 0. \end{aligned} \quad (12)$$

Substituting (12) into (11), we get

$$j_1 - j_2 = \frac{\mu_1 n_1 + \mu_2 n_2}{|e_1|} (e_1 E - \Phi \Omega) = 0, \quad (13)$$

where we have used $e_1 = -e_2$. Equation (13) is satisfied in two cases: $\mu_1 n_1 = \mu_2 n_2 = 0$ and $e_1 E - \Phi \Omega = 0$. In either case we obtain a contradiction with (12). Consequently, $j_1 = j_2 = 0$, and injection (1,2) is impossible.

The other cases of double injection can be studied in an analogous way. The result can be represented in the form of a matrix

$$\begin{pmatrix} - & - & + & + \\ - & - & + & + \\ + & + & - & - \\ + & + & - & - \end{pmatrix}, \quad (14)$$

where a plus or minus sign at the intersection of the i th column and j th row indicates the possibility or impossibility of the corresponding steady-state double injection. The physical meaning of these restrictions is very simple. For example, in the injection of carriers 1 and 2 their fluxes change the states of the bonds in an identical manner, leading to the unbounded growth of the configuration vector. In the final analysis their values will be sufficient to cancel the electric field in Eqs. (8), and the current will be cut off.

A similar investigation shows that any triple or quadruple steady-state injection is possible.

§3. Double steady-state injection (1,3) with a small initial defect concentration

In the steady one-dimensional case we have $j_1 = j_3 = j_0$, where j_0 is a constant. Assuming that the initial concentrations are small, $n_{i0} \ll \delta n_i$, and taking into account what was said above, we obtain from Eqs. (5), (7), and (8)

$$E' = \frac{4\pi}{\epsilon} (e_1 \delta n_1 + e_3 \delta n_3), \quad (15.1)$$

$$\Omega' = -\delta n_1 + \delta n_3, \quad (15.2)$$

$$(\Phi \Omega - e_1 E) \delta n_1 = -e_1 j_0 / \mu_1, \quad (15.3)$$

$$(\Phi \Omega + e_3 E) \delta n_3 = e_3 j_0 / \mu_3. \quad (15.4)$$

These equations should be supplemented with boundary condition (10). Eliminating δn_1 and δn_3 with the aid of (15.3) and (15.4), we easily obtain a single equation for $d\Omega/dE$ and a boundary condition for Ω and E at $x \rightarrow 0$. The only solution of this equation that satisfies the boundary condition is

$$\Omega = \frac{e_1 e_3 (\gamma_1 + \gamma_3) (u_1 - 1)}{\Phi (e_1 \gamma_1 - e_3 \gamma_3)} E, \quad (16)$$

where

$$u_1 = \frac{1-\theta}{2} + \left(\frac{(1-\theta)^2}{4} + \theta \Gamma \right)^{1/2}, \quad \gamma_i = |e_i| / \mu_i,$$

$$\theta = \frac{\epsilon \Phi}{4\pi e_1 e_3} \ll 1, \quad \Gamma = e^2 \gamma_1 \gamma_3 / e_1 e_3 (\gamma_1 + \gamma_3)^2.$$

Even this solution exists only for a single value of r :

$$r \approx \frac{\mu_1}{\mu_3} \left[1 - \theta \frac{e (\gamma_1 + \gamma_3) (\Gamma - 1)}{e_1 \gamma_1 - e_3 \gamma_3} \right]. \quad (17)$$

At other values of r there are no solutions.

Using (16) and (15), we easily find

$$E = (2d j_0 x)^{1/2}, \quad (18)$$

where

$$d = \frac{4\pi}{\epsilon} \left[\frac{(u_1 - 1) (e_1 \gamma_1 - e_3 \gamma_3)}{e_1 e_3} + \gamma_1 + \gamma_3 \right]$$

and from (4), (9), and (18) we obtain the current-voltage characteristics

$$I = 9eV^2 / 8dl^3. \quad (19)$$

Expanding d in powers of θ , we finally obtain

$$I = 9e\epsilon\mu_1\mu_3 V^2 / 32\pi (e_1\mu_3 + e_3\mu_1) l^3. \quad (20)$$

Formula (20) describes a typical volt-ampere characteristic for a space-charge-limited current, but with the high-

frequency dielectric constant ϵ instead of the static constant ϵ_s . In addition, if one of the mobilities μ_1 and μ_3 is much larger than the other, then the current is governed by the smaller mobility.

Further, from (15.3), (15.4), and (16) we find

$$\delta n_3 / \delta n_1 = r, \quad (21)$$

where r is given by Eq. (17). This result has a simple physical meaning. The presence of the configuration vector requires that $j_1 = j_3$. As a result, the concentrations adjust themselves so as to compensate the difference in the mobilities (to leading order in θ , one has $r \approx \mu_1 / \mu_3$). For this reason a solution satisfying the boundary conditions exists only at the fixed value of r given by formula (17).

In solving the problem we have used two conditions, viz., that the diffusion currents and initial concentrations are small. From (15.1), (18), and (21) we easily get

$$\delta n_i \approx j_i / \mu_i (2dj_0 x)^{1/2}. \quad (22)$$

Hence, the diffusion current $D_i n_i'$ is larger than the drift current j_i only for

$$x \ll (kT/eV)^{1/2} l, \quad (23)$$

i.e., in a narrow region near the contact, and, consequently, its contribution to the volt-ampere characteristic can be neglected. Further, the conditions $\delta n_i \gg n_{i0}$ are manifestly satisfied if

$$V \gg \frac{e}{\epsilon} \frac{\max\{\mu_i\}}{\min\{\mu_i\}} \max\{n_{i0}\} l^2. \quad (24)$$

§4. Double steady-state injection (1,3) with a large initial concentration of type 3 defects

Let us assume that the initial concentrations satisfy the conditions $\delta n_{1,3} \gg n_{10}, n_{20}, n_{40}$ and $\delta n_{1,3} \ll n_{30}$. This can be achieved by doping the ice with impurities which form type 3 defects or, if $n_{30} \gg n_{10}, n_{20}, n_{40}$, by decreasing the voltage V , i.e., decreasing $\delta n_{1,3}$.

A system of equations describing this case is obtained from system (15) by replacing δn_3 in Eq. (15.4) by n_{30} :

$$(\Phi\Omega + e_3 E) n_{30} = e_3 j_0 / \mu_3. \quad (25)$$

Because $\delta n_3 \rightarrow \infty$ at the boundary, Eq. (25) is violated near the $x = 0$ contact, where, as before, system (15) holds. Bearing this in mind, we shall solve Eqs. (15.1), (15.2), (15.3), and (25) using as a boundary condition the smooth joining with solution (18) at a point x_0 determined from the condition

$$\delta n_3 = j_0 / \mu_3 (2dj_0 x_0)^{1/2} = n_{30}. \quad (26)$$

Eliminating Ω , δn_3 , and δn_1 in succession, we obtain an equation for E :

$$(E - E_c) E' = b j_0, \quad (27)$$

where

$$E_c = e_3 j_0 / e \mu_3 n_{30}, \quad b = 4\pi e_1 / \epsilon \mu_1 (1 + 4\pi e_3^2 / \epsilon \Phi).$$

Hence we obtain for the field E

$$E = E_c + (2bj_0(x - x_0) + e_1^2 E_c^2 / e_3^2)^{1/2}. \quad (28)$$

If $x_0 \ll l$ (i.e., if n_{30} is large and j_0 is small) then, nearly throughout the entire crystal, we can use the expression

$$E = (2bj_0 x)^{1/2}, \quad (29)$$

which gives for the volt-ampere characteristic

$$I = 9eV^2 / 8bl^3. \quad (30)$$

With increasing voltage, x_0 increases, and at $x_0 \approx l$ we have the case examined in the previous section. In the intermediate case $x_0 \leq l$, assuming that we have solution (18) for $x < x_0$ and solution (29) for $x > x_0$, we can obtain the interpolation formula

$$I = 9eV^2 / 8 [(dx_0^3)^{1/2} + (bl^3)^{1/2}]^2, \quad (31)$$

where x_0 is given by (26). We have also used

$$\frac{d}{b} \approx \frac{\max\{\mu_1, \mu_3\}}{\mu_3 \epsilon \Phi} 4\pi e_3^2 \gg 1.$$

Figure 3 shows a schematic log-log plot of all of our results for the volt-ampere characteristics. In region *a* the voltage is so small that $\delta n_{1,3} \ll n_{10}, n_{30}$. In this case, as usual, we have ohm's law $I \propto V$. In region *b* the voltage is so large that the condition $n_{10}, n_{20}, n_{40} \ll \delta n_{1,3} \ll n_{30}$ holds, and we therefore have the quadratic behavior (30). The transition voltage from *a* and *b* yields an estimate of n_{10} , and from (30) we can find the mobility μ_1 . Finally, in the highest-voltage region *c* the condition $\delta n_{1,3} \gg n_{10}$ holds. The volt-ampere characteristic (20) is again quadratic, but with a different coefficient. The transition voltage from *b* to *c* makes it possible to estimate n_{30} , and from formula (20) one can obtain the mobility μ_3 if $\mu_3 \ll \mu_1$. If, on the other hand, $\mu_1 \ll \mu_3$, then, instead of the situation considered in Sec. 4, we must create a situation such that $n_{20}, n_{30}, n_{40} \ll \delta n_{1,3} \ll n_{10}$. We emphasize still another important distinction between the above results and the theory of electronic injection: In the present case, despite the small size of the injected concentrations $\delta n_{1,3}$ in comparison with the original concentration n_{30} (region *b*), the volt-ampere characteristic is quadratic, and not linear.

Let us estimate the applicability criterion for the results of Sec. 4. The diffusion current can be neglected if

$$\frac{\max\{\mu_1, \mu_3\}}{\mu_1} \frac{kT}{eV} \ll 1.$$

The conditions on the concentration give

$$10l^2 r_{00} n_{30} \gg \frac{eV}{kT} \gg 10l^2 r_{00} n_{10,20,40}.$$

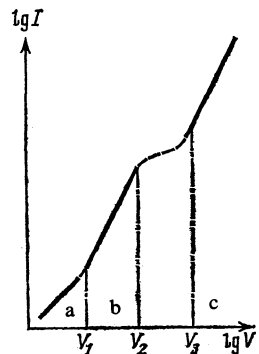


FIG. 3. Theoretical volt-ampere characteristics for ice samples with proton-injecting electrodes. For $V < V_1$ (region *a*) we have Ohm's law, while for $V_1 < V < V_2$ (*b*) and $V > V_3$ (*c*) we have $I \propto V^2$.

In concluding Part I we note that the results for the other types of double injection, e.g., (2.4), (1.4), and (2.3), can easily be obtained from the results of Secs. 3 and 4. In fact, everything reduces to a suitable change of indices. Thus the cases considered actually exhaust all the possible types of double injection.

PART II. EXPERIMENTAL RESULTS AND DISCUSSION

§1. Techniques

To obtain single-crystal samples of ice with a low initial concentration of current carriers we used thrice-distilled water which had been deionized by multiple passage through an Elga ion-exchange column and filtered through a $0.2\text{-}\mu\text{m}$ microfilter to eliminate the organic particles entering the water from the ion-exchange columns. The dissolved gases were eliminated by boiling under evacuation by a roughing pump at $T = 35^\circ\text{C}$ for 8–10 h. The resistivity of the prepared water was $(0.9\text{--}1.3) \cdot 10^7 \Omega \cdot \text{cm}$.

The ice crystals were grown in a large desiccator in a thermally insulated jacket at a temperature of -4.5°C . The geometry of the thermal insulation of the desiccator was such that the water froze from its surface into its interior at an average rate of 1 cm/day. The growth took place under continuous evacuation by a roughing pump. The single-crystal nature of the ice and the direction of the c axis were monitored by observing the birefringence.

The samples for the measurements were cut from the bars with a thin metal saw, sanded with an abrasive paper, and mechanically polished with filter paper. The thin ($\sim 50 \mu\text{m}$) work-damaged surface layer was then evaporated off. The samples were thin slabs 0.3–1.0 mm thick and about 5 cm^2 in area. The c axis lay in the plane of the slabs.

We used three types of contacts.

a) Proton-injecting contacts of a hydrogen-saturated palladium alloy (96% Pd + 4% Ag) in the shape of thin (1 mm) plates of area 1 cm^2 . The alloy was saturated either by cyclic oxidation and reduction in a hydrogen flame or by an electrochemical method from a 1 M aqueous solution of HCl at a current density of 0.03 A/cm^2 .

b) Blocking contacts of platinum foil.

c) Blocking contacts of a liquid In–Hg amalgam.

The rigid electrodes (Pd and Pt) were attached to the ice samples without melting by simple placing them in mechanical contact. Owing to the transport of material along the surface of the ice, after 2–5 h at $T = -4.5^\circ\text{C}$ a continuous contact was formed between the ice and the electrodes.

To eliminate surface currents we used a guard ring of In–Hg amalgam, as shown in Fig. 4. This figure also shows a block diagram of an arrangement which permitted simultaneous measurement of the volt-ampere characteristics, the frequency dependence of the capacitance $C(\omega)$ and conductance $G(\omega)$, and also the transient characteristics $C(\omega, t)$ and $G(\omega, t)$ upon application of square voltage pulses to the samples. The ac circuit was isolated from the high-voltage dc circuit by capacitors C_1 and C_2 ($\approx 5 \cdot 10^{-9} \text{ F}$), while resistors R_1 and R_2 ($\approx 3 \cdot 10^6 \Omega$) prevented short-circuiting of the bridge by the alternating current through the voltage source and electrometer. The ac bridge (General Radio 1615 A) per-

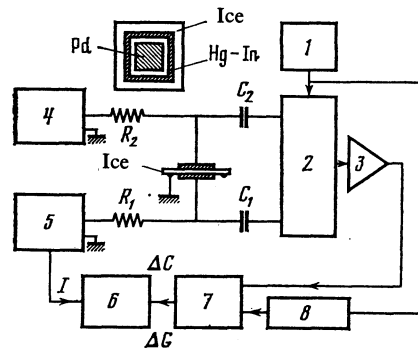


FIG. 4. Block diagram of the experimental apparatus: 1) oscillator, 2) ac bridge, 3) selective amplifier, 4) dc voltage source, 5) electrometer, 6) x-y recorder, 7) synchronous detector, 8) phase shifter.

mitted determination of the capacitance and conductance to an accuracy of $\Delta C = \pm 10^{-3} \text{ pF}$, $\Delta G = \pm 10^{-10} \text{ mho}$ at $f = 10^5 \text{ Hz}$ and $\Delta C = \pm 1 \text{ pF}$, $\Delta G = \pm 5 \cdot 10^{-10} \text{ mho}$ at $f = 20 \text{ Hz}$.

The measurements were made at temperatures T between -4 and -56°C , frequencies f between 20 and $2 \cdot 10^5 \text{ Hz}$, and dc voltages V between 0.01 and $3 \cdot 10^3 \text{ V}$. The amplitude of the alternating voltage did not exceed 1% of the dc voltage.

§2. Results and discussion

Figures 5–8 show the experimental results necessary for comparison with the theoretical formulas.

The results shown in Figs. 5 and 6 are of the form which one would expect in the case of an easy exchange of protons between the sample and the contact. In fact, the dispersion curve for the case without a dc voltage has the ideal Debye shape implied by the Jaccard theory for a free exchange of carriers between the sample and the contacts.¹⁰ For blocking contacts the dispersion curve (see Fig. 7) differs from the Debye curve by the presence of low-frequency dispersion, which is due to the accumulation of carriers near the contacts and the formation of inhomogeneities. This low-frequency dispersion can take extremely complex forms¹⁵; these forms were explained theoretically and used to study the electrical properties of ice in Ref. 16. A dc voltage ap-

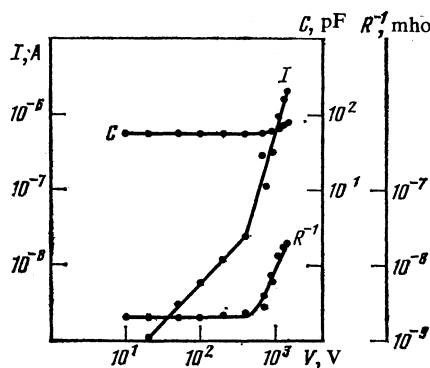


FIG. 5. Plots of the direct current I , inverse resistance R^{-1} (120 Hz), and capacitance C (120 Hz) of an ice sample with two hydrogen-saturated palladium electrodes; $T = -16^\circ\text{C}$; sample thickness 0.7 mm.

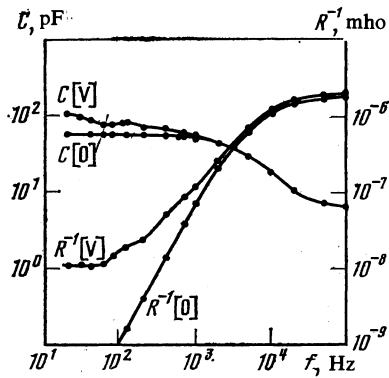


FIG. 6. Influence of dc voltage V on the frequency dependence of the capacitance C and inverse resistance R^{-1} of a sample with two palladium electrodes; $T = -16^\circ\text{C}$; $V = 2\text{ kV}$; sample thickness 0.7 mm .

plied to a sample with palladium contacts creates a nonuniform carrier distribution, and this is reflected in the low-frequency part of the dispersion curve (additional dispersion arises). A dc voltage applied to a sample with platinum contacts causes the dispersion curves to approach the Debye curve; this can actually indicate a shift of the low-frequency dispersion to lower frequencies.

Finally, it is seen in Fig. 5 that the deviation of the volt-ampere characteristics from ohmic is correlated with an increase in the high-frequency conductance. Furthermore, as is seen in Fig. 6, a high dc voltage increases R^{-1} over the entire frequency range, indicating an increase in the carrier concentration.

All the aforementioned facts thus indicate that the deviation of the volt-ampere characteristics from ohmic at $V = 400\text{ V}$ is due to the injection of protons and to an increase in their volume concentration, rather than to nonlinear properties of the contacts.

Let us now turn to a comparison of the experimental results with the theoretical formulas obtained in Part I. The results on the effects of doping on the electrical properties of ice imply that in pure ice the majority carriers are L defects and the minority carriers are H_3O^+ defects. Consequently, the high-frequency conductivity is given by

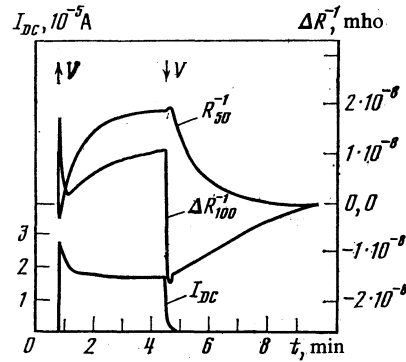


FIG. 8. Transient characteristics of a sample with two proton-injecting palladium contacts upon application of a square voltage pulse $V = 1.86\text{ kV}$; $T = -15^\circ\text{C}$, sample thickness 0.55 mm ; I_{DC} is the dc current, R_{50}^{-1} and R_{100}^{-1} are the inverse resistances at frequencies of 50 kHz and 100 Hz , respectively.

$$\sigma_\infty = \sigma_1 + \sigma_4 \approx \sigma_4, \quad (32)$$

i.e., is governed by the L defects. For the low-frequency conductivity we have

$$\frac{1}{\sigma_0} = \left(\frac{e_4}{e}\right)^2 \frac{1}{\sigma_4} + \left(\frac{e_1}{e}\right)^2 \frac{1}{\sigma_1} \approx \left(\frac{e_1}{e}\right)^2 \frac{1}{\sigma_1}, \quad (33)$$

i.e., σ_0 is governed by the H_3O^+ ions.¹² As the dc voltage is increased, σ_0 and σ_∞ monotonically increase. Consequently, it can be supposed that in the present case we are dealing with the injection of H_3O^+ and L defects. Here it follows from Figs. 5 and 6 that $\sigma_0 \ll \delta\sigma_0 \ll \sigma_\infty$, $\sigma_\infty \gg \delta\sigma_\infty$, or $\delta n_1 \gg n_{10}$, $\delta n_4 \gg n_{10}$, $\delta n_{1,4} \ll n_{40}$. The injection in this case is described by the formulas of Sec. 4 if it is recognized that $e_3 = -e_4$ and $\eta_3 = -\eta_4$. From Eqs. (27) and (30) we have

$$\mu_1 = 8e_1^2 I / 9eV^2 C_0, \quad (34)$$

where C_0 is the low-frequency capacitance with

$$\epsilon_0 = \epsilon(1 + e_4^2 / 4\pi\epsilon\Phi). \quad (35)$$

We obtain the concentrations from (33) as

$$n_{10} = \sigma_1 / e_1 \mu_1 = \sigma_0 (e_1 / e)^2 / e_1 \mu_1 = \sigma_0 e_1 / \mu_1 e^2. \quad (36)$$

For the volt-ampere characteristics that are nearly quadratic (the deviations from quadratic volt-ampere characteristics in several samples are apparently due to the presence of traps in those samples), calculations with Eqs. (34) and (36) yield the following values at a temperature of -20°C :

$$\mu_1 \approx (1-6) \cdot 10^{-4} \text{ cm}^2 / \text{V} \cdot \text{sec}, \quad n_{10} \approx 10^{10} - 10^{14} \text{ cm}^{-3}.$$

The spread in these values can be attributed to the influence of traps, which decrease the current and thereby cause an apparent decrease in μ_1 . The value $6 \cdot 10^{-4} \text{ cm}^2 / \text{V} \cdot \text{sec}$ should thus be considered a lower value of the mobility of H_3O^+ defects.

We have so far been unable to reach the second quadratic region on the volt-ampere characteristics (see Fig. 3). To reach this region, from which one can determine n_{40} and μ_4 , it will be necessary to go to lower temperatures and thinner samples.

Finally, there is an interesting property of the transient characteristics that can be interpreted as confirmation of type

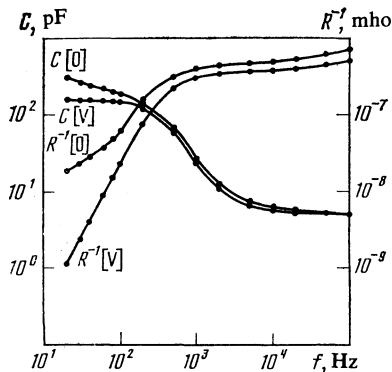


FIG. 7. Influence of dc voltage V on the frequency dependence of C and R^{-1} of a sample with two blocking electrodes of Pt; $T = -30^\circ\text{C}$; $V = 1.5\text{ kV}$; sample thickness 0.56 mm ; electrode area 1 cm^2 .

(1,4) injection. By injecting protons from the right-hand contact, we form H_3O^+ and D defects. The D defects, annihilating with L defects, decrease the concentration of the latter and thereby decrease σ_∞ , as is seen in Fig. 8. Then the H_3O^+ ions reach the left-hand, negative contact and give off a proton; in other words, the H_3O^+ ions are destroyed and L defects are formed. The latter move into the sample and on the right-hand contact annihilate with injected D defects. At this time the high-frequency conductivity starts to grow again. The motion of L defects rather than D defects in the sample is apparently due to their higher mobility.

¹W. H. Barnes, Proc. Roy. Soc. A **125**, 670 (1925).

²P. G. Owston, Adv. Phys. **7**, 171 (1958).

³J. D. Bernal and R. H. Fowler, J. Chem. Phys. **1**, 515 (1933).

⁴L. Pauling, J. Am. Chem. Soc. **57**, 2680 (1935).

⁵J. F. Nagle, J. Math. Phys. **7**, 1484 (1966).

⁶W. F. Gisuque and J. W. Stout, J. Am. Chem. Soc. **58**, 1144 (1936).

⁷N. K. Bjerrum, K. Dan. Vidensk. Selsk. Mat.-Fys. Medd. **27**, 56 (1951).

⁸H. Gränicher, Z. Kristallogr. Kristallgeom. Kristallphys. Kristallchem. **110**, 432 (1958).

⁹C. Jaccard, Helv. Phys. Acta **32**, 89 (1959).

¹⁰C. Jaccard, Phys. Kondens. Mater. **3**, 99 (1964).

¹¹M. Hubmann, Z. Phys. B **127**, 141 (1979).

¹²P. V. Hobbs, Ice Physics, Clarendon Press, Oxford (1974).

¹³M. A. Lampert and P. Mark, Current Injection in Solids, Academic Press, New York (1970).

¹⁴K. C. Kao and W. Hwang, Electrical Transport in Solids, Pergamon Press, Oxford (1981).

¹⁵A. von Hippel, A. H. Runk, and W. B. Westphal, Physics and Chemistry of Ice (ed. by E. Walley, S. J. Jones, and L. W. Gold), Royal Society of Canada, Ottawa (1973), p. 236.

¹⁶V. F. Petrenko and I. A. Ryzhkin, Phys. Status Solidi B **121**, 421 (1984).

Translated by Steve Torstveit